ROTOR-BEARING ANALYSIS OF A SINGLE SPOOL GAS TURBINE BY USING THE FINITE ELEMENT METHOD

Geraldo Creci Filho, gcreci@ita.br
João Carlos Menezes, menezes@ita.br
Instituto Tecnológico de Aeronáutica – São José dos Campos – SP

José Francisco de Castro Monteiro, monteiro@iea.cta.br
Instituto de Aeronáutica e Espaço – São José dos Campos – SP

João Aparecido Corrá, joaocorra@tgmturbinas.com.br
TGM Turbinas Ltda – Sertãozinho – SP

Abstract. *Nowadays, the development of gas turbines is becoming more and more important due to the fact that gas turbines can be used in aeronautical applications and in electric power generation systems. Less pollutant fuels, such as biodiesel and alchool, can be easily adapted to run on gas turbines, instead of traditional kerosene. In this paper, the dynamic behaviour of a single spool gas turbine is investigated. The main rotor-shaft of the studied gas turbine is supported on two bearings: a deep groove ball bearing and a squeeze film damper. The stiffness and damping dynamic properties of these two bearings are used to perform a full rotordynamic analysis on the system. A finite element model belonging to a C^l-class formulation is used for the study of whirl speeds and unbalance response analyses. Modal orbits of the shaft are exhibited in the frequencies of major interest. Additionally, a transient analysis is performed to simulate the transition of the system through the most important ressonance points. As a result, the dynamic behaviour of the rotor-bearing system is predicted and vibration problems are avoided. The good convergence and high accuracy of the results are demonstrated with several numerical analyses.*

Keywords: rotordynamic analysis, gas turbines, finite element method, critical speeds, transient analysis.

1. INTRODUCTION

A full rotordynamic analysis is mandatory to avoid vibration resonance for a gas turbine operation with high speed. The critical speeds are defined as coincidence of the shaft rotating speed and the rotating natural frequencies of the rotor-bearing system. Since catastrophic failure is found at critical speeds due to resonance, the critical speeds are designed by separating them sufficiently from the operating speed range. The determination of instability threshold and unbalance response of the system are also subjects of major concern.

There are several numerical approximations for vibration analysis of rotor-bearing systems. The most popular approach which is particularly well suited for modeling large scale and complicated systems is the finite element method. Historically, Ruhl and Booker (1972) are probably the first to utilise the finite element method to study the stability and unbalance response of turbo-rotor systems. In their finite element formulation, only elastic bending energy and translational kinetic energy were included. Nelson and McVaugh (1976) generalized the formulation by considering the effects of rotary inertia, gyroscopic moments and axial loads to model a flexible rotor system supported on linear stiffness and viscous damper bearings. In the work of Zorzi and Nelson (1977), both internal viscous and hysteretic damping were included in the formulations. Afterwards, Nelson (1980) utilised Timoshenko beam theory for establishing shape functions and, thereby included shear effects.

More recently, Lalanne and Ferraris (2001) presented a systematic and pratical approach to the analytical and numerical aspects of the prediction of rotordynamics behaviour. Large scale and more complicated models were successfully analysed. Kalita and Kakoty (2004) presented an analysis of whirl speeds for rotor-bearing systems supported on fluid film bearings. It was observed in their analyses the presence of a half-frequency whirling, which could potentially cause subharmonic instabilities on the system. Chiang *et al.* (2004) presented several analyses applied to both single-rotor and dual-rotor systems. In the dual-rotor application, the effects of the speed ratio of the high-speed to low-speed shafts on the critical speeds was studied. Young *et al.* (2007) investigated the lateral vibration of a spinning disk-shaft system supported by a pair of ball bearings and subjected to random axial forces. The random axial forces simulated external reactions at both ends of the rotor. In such situation, the rotor-bearing system may experience parametric random instability. Wu (2007) studied how to predict the lateral vibration characterists of the full-size rotor-bearing system by using the scaling rotor-bearing model and the associated scaling laws. In his work it is presented a systematic theory to validate theroretical results with experimental data using scale models. The use of scale models can significantly reduce costs and save time during the product design phase.

Another important issue on rotordynamics reffers to the reduction of vibration levels. Strauss *et al.* (2007) studied the reduction of the vibration levels by design optimization. The mass fuction is used as the objective function of the optimization problem and constraints are set on the nonlinear and nonconvex functions of critical speed and unbalance

responce. Jeon *et al*. (2008) studied a practical engineering problem. They used a three-dimensional finite element method to perform a critical speed analysis over a 30-ton thrust demonstrator turbopump considering the casing structural flexibility. Another real application was studied by Combescure and Lazarus (2008). They presented a refined finite element modelling of a gas turbine modular helium reactor power convertion unit. Stability and forced response analysis were performed taking into account the flexibilities not represented by a beam model.

In this paper, the rotordynamic behaviour of a single spool gas turbine is investigated. A finite element model belonging to a C^1-class formulation is used for the study of whirl speeds and unbalance response analyses. Modal orbits of the shaft are plotted in the frequencies of major interest and a transient analysis is performed to simulate the transition of the system through the most troublesome ressonance points. The good convergence and high accuracy of the results are demonstrated with several numerical analyses.

2. ROTORDYNAMIC MODEL

The single spool gas turbine studied in this work has been developed for unmanned aerial vehicle applications. Figure 1 shows a half-section view of the studied gas turbine designed to produce 5 kN of thrust at 28,150 rpm. This gas turbine is composed by a five-stage axial compressor, an annular combustion chamber and a single-stage turbine rotor. Several excitation frequencies can be originated by the rotor speed ω. The most critical is the mass unbalance of the rotor in the frequency ω. Coupling misalignments give origin to excitation frequencies $2*\omega$. Blade, vanes, nozzle, diffuser and other devices produce excitation frequencies $s*\omega$; where s is the number of blades, vanes and so on. Aerodynamic excitations are also of interest. They produce excitation frequencies $0.5*\omega$.
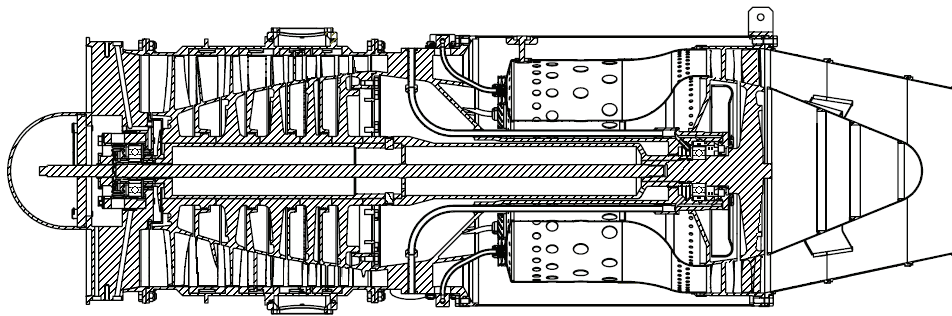

Figure 1. Half-section view of the studied single spool gas turbine.

The main rotor-shaft of the studied gas turbine is supported on two bearings: a deep groove ball bearing and a squeeze film damper. In the works of Creci *et al*. (2009a) and Creci *et al*. (2009b), the stiffness and damping dynamic properties of these two bearings are calculated. The front bearing of the gas turbine is composed by a 206(T) Barden® deep groove ball bearing. The rear bearing of the gas turbine is an unsealed squeeze film damper with a circumferential feeding groove. The calculated stiffness and damping dynamic properties of the front bearing is presented in Fig. 2(a). The calculated stiffness and damping dynamic properties of the rear bearing is presented in Fig. 2(b). In the finite element model, the calculated stiffness and damping values are used as $K_{xx}=K_{yy}$ and $C_{xx}=C_{yy}$. The stiffness and damping cross values are considered to be null; i.e., $K_{xy}=K_{yx}=C_{xy}=C_{yx}=0$.
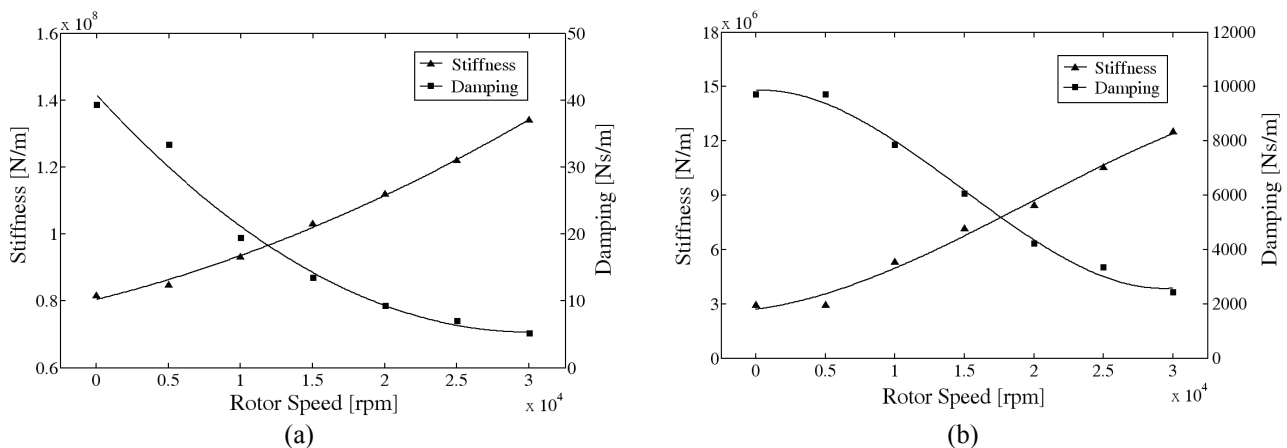

(a) (b)

Figure 2. (a) Stiffness and damping dynamic properties of the front bearing of the single spool gas turbine;
(b) Stiffness and damping dynamic properties of the rear bearing.

Figure 3 shows the rotor-bearing model of the studied gas turbine. The rotor-shaft is made of AISI 4340 steel. The Young's modulus of AISI 4340 steel is 205 GPa, the Poisson's ratio is 0.29, and the density is 7850 kg/m^3. The rotor-discs are made of different materials to withstand the variations of mechanical stresses and thermal loads. Table 1 shows the main physical and geometric properties of the rotor-discs. The first three discs of the axial compressor are made of aluminium alloys. The forth and fifth discs are made of titanium alloy, since the temperatures over these discs are significantly higher. The sixth disc is the free turbine rotor, which is made of inconnel alloy. This rotor-disc is subjected to high temperatures loads originated by the post-combustion gases.
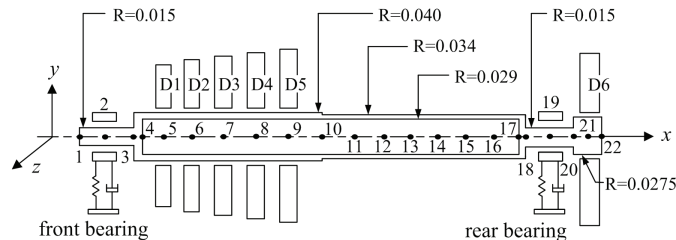

Figure 3. Rotor-bearing model of the studied gas turbine.

Table 2 shows the location of the principal nodes of the finite element model. The Ansys® software is used as the solver for the numerical analyses. The shaft is modeled by the Beam189 element. The Beam189 element has three nodes and each node has four degrees of freedom: two translations and two rotations. The rotor-discs are modeled by the Pipe16 element. The front and rear bearings of the gas turbine are modeled by the Combin14 and Matrix27 elements. The Matrix27 element is used because the stiffness and damping dynamic properties of the bearings vary nolinearly with rotor speed increasing. The stiffness and damping data are stored in tables.

The Ansys® solver uses a C^1-class finite element formulation since the Timoshenko beam theory is used for establishing the shape functions, and based on these shape functions the system finite element matrices of governing equations are derived. In these system finite element matrices, a shear parameter Φ is included in the shape functions to consider the effect of transverse shear deformations. The internal viscous damping of the model is assumed to be 4 s^{-1}. The harmonic and transient analyses were performed considering an unbalance of 0.0001 kg.m situated at node 21.

Table 1. Physical and geometric properties of the rotor-discs.

	D1	D2	D3	D4	D5	D6
Material	Al7178-T6	Al7178-T6	Al2024-T81	Ti-6Al-4V	Ti-6Al-4V	In713LC
Young's modulus, [GPa]	71.7	71.7	72.4	113.8	113.8	163.3
Density, [kg/m^3]	2830	2830	2870	4430	4430	8000
Poisson's ratio	0.33	0.33	0.33	0.342	0.342	0.382
Width, [m]	0.02	0.02	0.02	0.02	0.02	0.03
Inner diameter, [m]	0.08	0.08	0.08	0.08	0.08	0.055
Outer diameter, [m]	0.19	0.21	0.23	0.24	0.25	0.25

Table 2. x-coordinates of the principal nodes of the finite element model.

Nodes	N1	N2	N3	N4	N5	N6	N7	N8
x, [m]	0	0.04	0.075	0.087	0.1	0.157	0.21	0.253
	N9	N10	N17	N18	N19	N20	N21	N22
	0.292	0.360	0.630	0.642	0.7	0.735	0.765	0.78

3. RESULTS AND DISCUSSIONS

The finite element model has 44 elements: 22 Beam189 elements, 06 Pipe16 elements, 04 Combin14/Matrix27 elements, and 12 Contact elements. The rotor-bearing system is designed to generate 5 kN of thrust at 28,150 rpm. The numerical analyses were performed considering a speed range from 0 to 30,000 rpm. The operating speed range is defined from 22,520 to 28,150 rpm, which means 80 to 100% of maximum allowable speed.

Figure 4 shows the Campbell diagram of the system and no instability occurs. Two critical speeds are of major concern: 1FW at 51.58 Hz and 2FW at 211.43 Hz. It can also be observed that the 3FW mode varies significantly with rotor speed increasing. The operating speed range is delimitated by the two dotted lines. There are no critical speeds over this region. Figure 5 shows the modal orbits of the shaft plotted in frequencies of major interest.
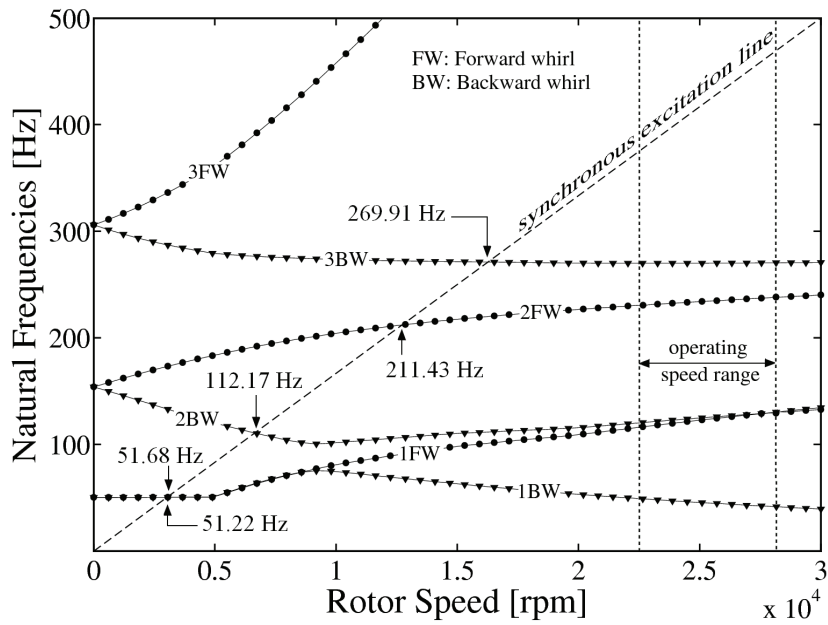
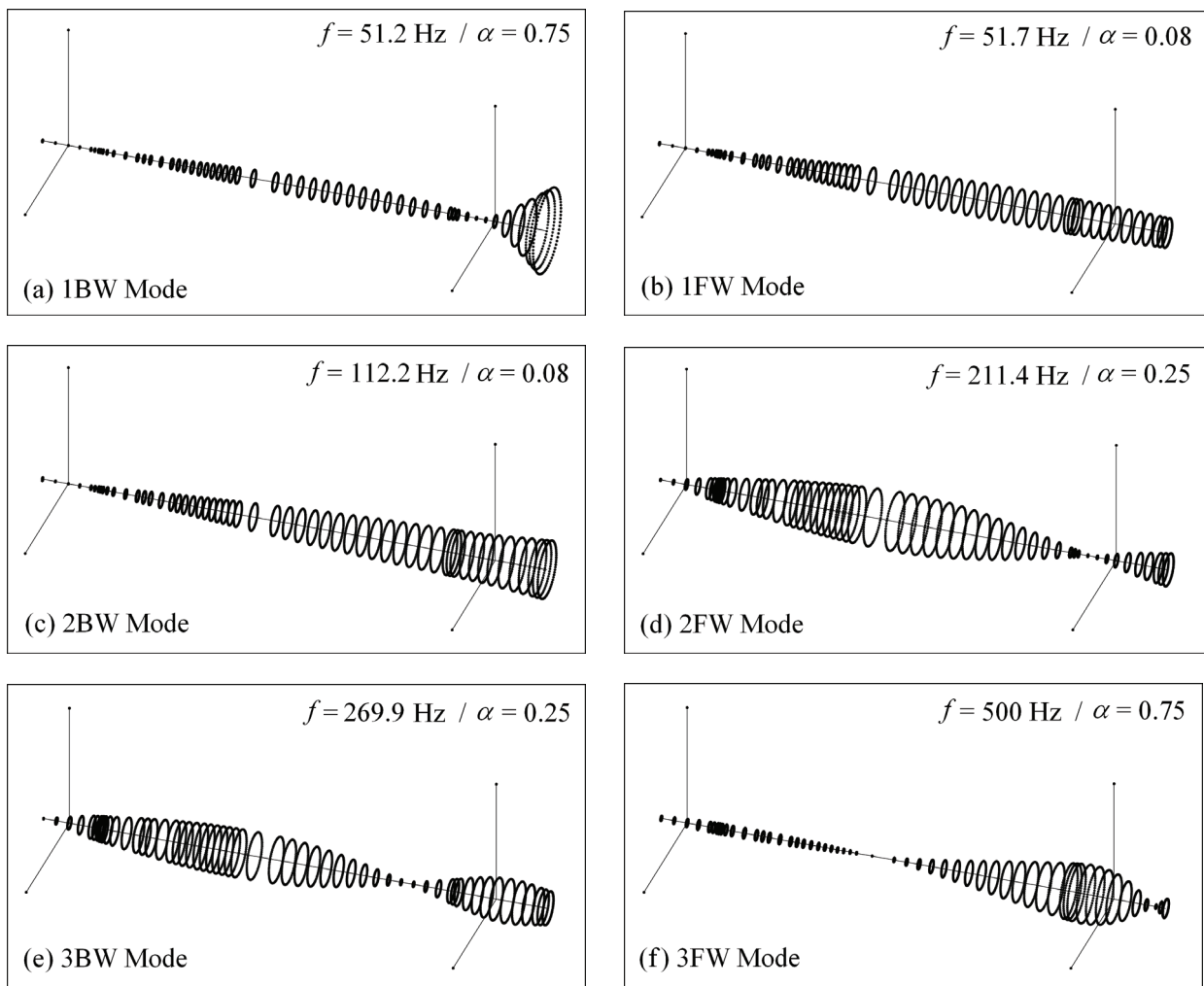Figure 4. Campbell diagram of the gas turbine rotor-bearing system.

Figure 5. Modal orbits of the shaft plotted in the frequencies of major interest.
The parameter α is a magnifying view factor.

A balance quality grade G2.5 is adopted from ISO standard 1940/1 to assure the balance quality of the rotor. In the numerical analyses, a mass unbalance of 0.0001 kg.m is placed at node 21 of the rotor-bearing system. Figures 6(a) and 6(b) show the unbalance responses of the system. It can be observed that the 2FW at 211.43 Hz critical speed is the most significative. The first critical speed 1FW at 51.58 Hz was dramatically attenuated by the damping characteristics of the rear bearing. No significative amplitude peak can be observed for the first critical speed in Figs. 6(a) and 6(b).

The unbalance responses of nodes 5, 7, 9 and 10 are shown in Fig. 6(a). These nodes were monitored to verify the amplitudes of vibration over the axial compressor region. The compressor region is a very critical region because the tip clearances of the blades are specified so small as possible to assure the component efficiency. From this design requirement, it is possible to note that large amplitudes of vibration over this region are not allowable. From Fig. 6(a) it is possible to note that vibration amplitudes over the compressor region do not reach 2 μm at the operating speed range.

The unbalance responses of nodes 20, 21 and 22 are shown in Fig. 6(b). These nodes were monitored to verify the amplitudes of vibration over the free turbine rotor. The turbine rotor is one of the most critical components since it is a free rotor and it is subjected to rigorous service conditions. The same consideration for the tip blade clearances is valid for this rotor. From Fig. 6(b) it is possible to observe that vibration amplitudes over the free turbine rotor do not reach 10 μm, also considering the operating speed range from 22,520 to 28,150 rpm.
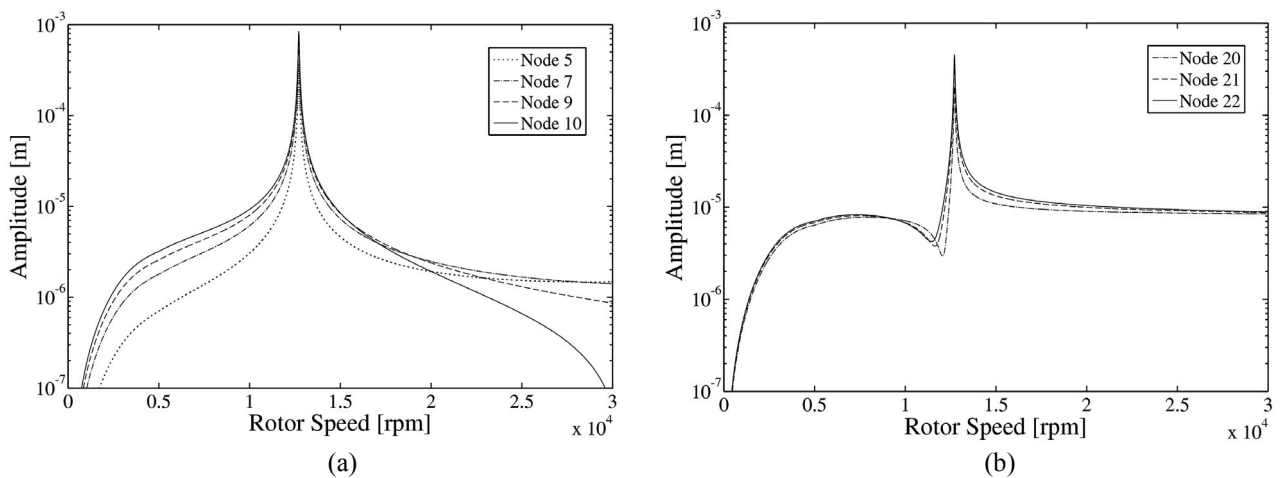

Figure 6. (a) Unbalance responses of nodes 5, 7, 9 and 10; (b) Unbalance responses of nodes 20, 21 and 22.

A transient analysis was performed to simulate the transition of the studied rotor-bearing system through the most critical resonance points. In the book of Lalanne and Ferraris (2001), several transient analyses are shown using different rotor-bearing configurations. In the present work, it was assumed a linear acceleration law followed by a constant speed of rotation. It was assumed an angular acceleration of 314.15 rad/s². The unbalance of 0.0001 kg.m is at node 21. Figure 7 shows the results for a 10 seconds total simulation time. The response is also measuared at node 21.
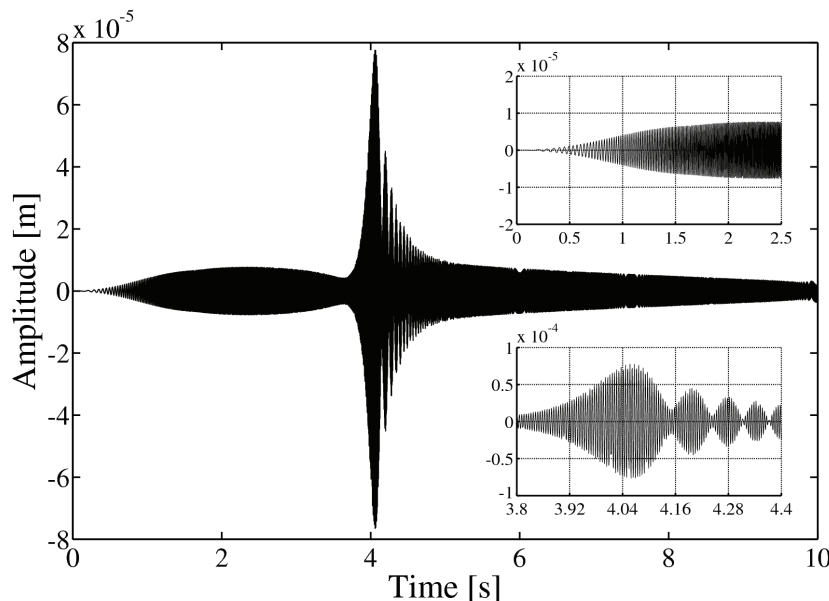

Figure 7. Transient analysis of the rotor-bearing system simulating the transition through the resonance points.

The results obtained are in good agreement with the unbalance response analyses previously presented. It can be observed that the 2FW at 211.43 Hz critical speed is the most troublesome. The 1FW at 51.58 Hz critical speed is strongly attenuated by the damping properties of the rear bearing, as can be seen in the period from 0 to 2.5 seconds.

Another good tool to observe the dynamic behaviour of a rotor-bearing system is the spectral map plot. Figure 8 shows a spectral map plot of the studied rotor-bearing system. The rotor speed ranges from 0 to 500 Hz with 50 substep solutions. The excitation frequency ranges from 0 to 500 Hz with 250 substep solutions. The vibration amplitudes are calculated using clusters with 5 Hz for bandwith and 0.5 Hz for minimum frequency. A good agreement with the previous analyses can be observed.

The largest amplitudes of vibration are due to the 2FW at 211.43 Hz critical speed. A small peak can be observed when the rotor speed is at 500 Hz and the excitation frequency is about 130 Hz. This peak illustrates the first critical speed of the system, which could not be observed in the previous analyses. The magnitude of the vibration amplitudes are in good agreement with the unbalance response analyses. Figure 6(b) shows that the maximum amplitude of vibration at node 21 is 0.0003712 m. In the spectral map plot shown in Fig. 8, it can be noted that the maximum value measuared at node 21 is 0.00037 m. This represents a numerical error smaller than 0.33%.
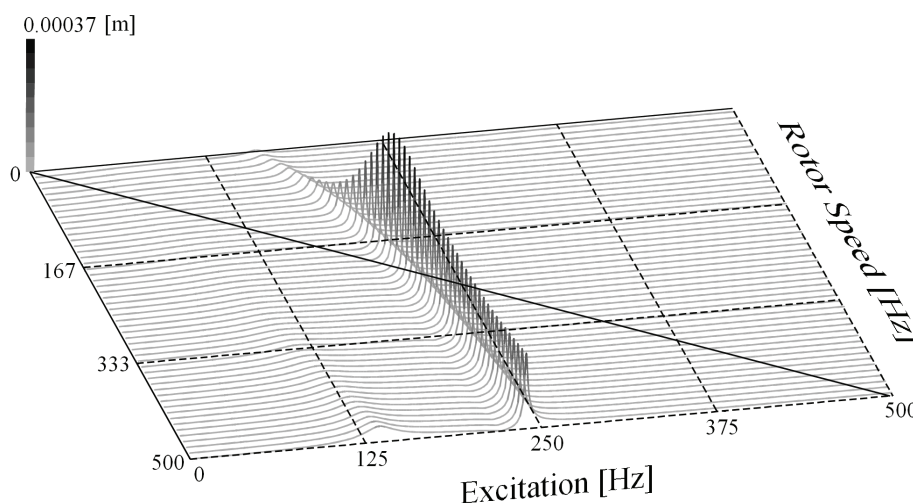

Figure 8. Spectral map plot of the studied gas turbine rotor-bearing system.

4. CONCLUSIONS

A full rotordynamic analysis over the investigated single spool gas turbine was successfully performed. There are relatively few works available in literature which take into account the effects of stiffness and damping dynamic properties of the bearings. In the finite element model presented in this work, the dynamic properties of the bearings are included in the formulations as a function of the rotor speed.

It can be observed a potentially troublesome resonance at about 12,686 rpm of rotor speed. This is the 2FW at 211.43 Hz critical speed. However, the operating speed range of system is specified from 22.520 to 28,150 rpm.

The vibration amplitudes of the compressor discs were monitored using the nodes 5, 7, 9 and 10 of the finite element model. It was observed that the vibration amplitudes of these nodes do not reach 2 μm at the operating speed range. The vibration amplitudes of the free turbine rotor were monitored using the nodes 20, 21 and 22. It was observed that the vibration amplitudes of these nodes do not reach 10 μm at the operating speed range.

Several numerical analyses were performed to demonstrate the high accuracy and good convergence of the results. The dynamic behaviour of the rotor-bearing system is predicted and no potential vibration problems are expected to happed when the turbine is running at the operating speed range.

The presented results may be of interest to the designers and researchers. The finite element model was carefully developed. Nevertheless, the observations made here from the theoretical analyses should have experimental verification, which was not possible at the present time due to unavailability of test rig.

5. ACKNOWLEDGEMENTS

6. REFERENCES

Chiang, H-W.D., Hsu, C-N. and Tu, S-H., 2004, "Rotor-Bearing Analysis for Turbomachinery Single- and Dual-Rotor Systems," AIAA, Journal of Propulsion and Power, Vol. 20, No. 6, pp. 1096-1104.

Combescure, D., Lazarus, A., 2008, "Refined Finite Element Modelling for the Vibration Analysis of Large Rotating Machines: Application to the Gas Turbine Modular Helium Reactor Power Convertion Unit," Journal of Sound and Vibration, Vol. 318, pp. 1262-1280.

Creci, G., Menezes, J.C., Monteiro, J.F.C. and Corrá, J.A., 2009a, "Investigation into the Dynamic Behaviour of a Lubricated Radial Ball Bearing using the EHL Contact Theory," Proceedings of the 8th Brazilian Conference on Dynamics, Control and Applications, Bauru-SP.

Creci, G., Menezes, J.C.. and Corrá, J.A., 2009b, "Dynamic Characteristics of an Unsealed Squeeze Film Damper with a Circumferential Feeding Groove," Proceedings of the XXXII Brazilian Congress on Computational and Applied Mathematics (Accepted for Publication), Cuiabá-MT.

Jeon, S.M., Kwak, H.D., Yoon, S.H. and Kim, J., 2008, "Rotordynamic Analysis of a Turbopump with the Casing Structural Flexibility," AIAA, Journal of Propulsion and Power, Vol. 24, No. 3, 433-436.

Kalita, M., Kakoty, S.K., 2004, "Analysis of Whirl Speeds for Rotor-Bearing Systems Supported on Fluid Film Bearings," Mechanical Systems and Sygnal Processing, Vol. 18, pp. 1369-1380.

Lalanne, M., Ferraris, G., 2001, "Rotordynamics Prediction in Engineering", 2nd ed., Wiley, New York, Chaps. 7 and 8.

Nelson, H.D., 1980, "A Finite Rotating Shaft Element using Timoshenko Beam Theory," ASME, Journal of Mechanical Design, Vol. 102, pp. 793-803.

Nelson, H.D., McVaugh, J.M., 1976, "The Dynamics of Rotor-Bearing Systems using Finite Elements," ASME, Journal of Engineering for Industry, Vol. 98, pp. 593-600.

Ruhl, R.L., Booker, J.F., 1972, "A Finite Element Model for Distributed Parameter Turbo Rotor Systems," ASME, Journal of Engineering for Industry, Vol. 94, pp. 128-132.

Strauss, F., Inagaki, M. and Starke, J., 2007, "Reduction of Vibration Level in Rotordynamics by Design Optimization," Structural and Multidisciplinary Optimization, Vol. 34, pp.139-149.

Young, T.H., Shiau, T.N. and Kuo, Z.H., 2007, "Dynamic Stability of Rotor-Bearing Systems subjected to Random Axial Forces," Journal of Sound and Vibration, Vol. 305, pp. 467-480.

Wu, J-J., 2007, "Prediction o Lateral Vibration Characterisitcs of a Full-Size Rotor-Bearing System by using those of its Scale Models", Finite Elements in Analysis and Design, Vol. 43, pp.803-816.

Zorzi, E.S., Nelson, H.D., 1977, "Finite Element Simulation of Rotor-Bearing Systems with Internal Damping," ASME, Journal of Engineering for Power, Vol. 99, pp. 71-76.

7. RESPONSIBILITY NOTICE

The authors are the only responsible for the printed material included in this paper.